J Mol Model (2012) 18:5075–5088
DOI 10.1007/s00894-012-1503-3

ORIGINAL PAPER

A joint experimental and theoretical investigation of kinetics and mechanistic study in a synthesis reaction between triphenylphosphine and dialkyl acetylenedicarboxylates in the presence of benzhydrazide

Mohammad Amin Kazemian · Sayyed Mostafa Habibi-Khorassani · Ali Ebrahimi · Malek Taher Maghsoodlou · Peyman Mohammadzadeh Jahani · Mahbobeh Ghahramaninezhad

Received: 8 April 2012 / Accepted: 11 June 2012 / Published online: 3 July 2012

Abstract Stable crystalline phosphorus ylides were obtained in excellent yields from the 1:1:1 addition reaction between triphenylphosphine (TPP) and dialkyl acetylenedicarboxylates, in the presence of NH-acids, such as benzhydrazide. To determine the kinetic parameters of the reactions, they were monitored by UV spectrophotometery. The second order fits were automatically drawn and the values of the second order rate constant (k_2) were calculated using standard equations within the program. At the temperature range studied the dependence of the second order rate constant (Ln k_2) on reciprocal temperature was compatible with Arrhenius equation. This provided the relevant plots to calculate the activation energy of all reactions. Furthermore, useful information were obtained from studies of the effect of solvent, structure of reactants (different alkyl groups within the dialkyl acetylenedicarboxylates) and also concentration of reactants on the rate of reactions. On the basis of experimental data the proposed mechanism was confirmed according to the obtained results and a steady state approximation and the first step (k_2) and third (k_3) steps of the reactions were recognized as the rate determining steps, respectively. In addition, three speculative proposed mechanisms were theoretically investigated using quantum mechanical calculation. The results, arising from the second and third speculative mechanisms, were far from the experimental data. Nevertheless, there was a good agreement between the theoretical kinetic data, emerge from the first speculative mechanism, and experimental kinetic data of proposed mechanism.

Keywords Kinetic parameters · NH-acid (benzhydrazide) · Stable phosphorus ylides · Transition state · Triphenylphosphine · UV spectrophotometery

M. A. Kazemian · S. M. Habibi-Khorassani (✉) · A. Ebrahimi · M. T. Maghsoodlou · P. M. Jahani · M. Ghahramaninezhad
Department of Chemistry, University of Sistan and Baluchestan, P. O. Box 98135-674, Zahedan, Iran
e-mail: smhabibikh@gmail.com

Introduction

Development of simple synthetic routes for widely-used organic compounds from readily available reagents is one of the major tasks in organic chemistry [1]. Phosphorus ylides are reactive systems, which take part in many valuable reactions of the organic synthesis [2–20]. These are most often prepared by treatment of a phosphonium salt with a base. Most of the phosphonium salts are usually made from phosphine and an alkyl halide [3–6] and they are also obtained by the Michael addition of phosphorus nucleophiles to activated olefins [2, 3]. In continuation of our previous works, herein benzhydrazide has been employed in an efficient synthetic route along with a joint experimental and theoretical study of kinetics and mechanism for reaction between triphenylphosphine and dialkyl acetylendicarboxylate to lead hydrazide derivatives as potentially peroxidase inhibitors. Arylhydrazines are oxidized by haem peroxidases to highly reactive radical species that can be incorporated at the active site [21]. Covalent haem modification by hydrazines (R-NH-NH2) has been employed as a method for probing active-site topology in a number of peroxidases [21–24]. Hydrazides (R-CO-NHNH2) are related compounds, and are known to be peroxidase inhibitors [25, 26]. Several hydrazine and hydrazide derivatives have been

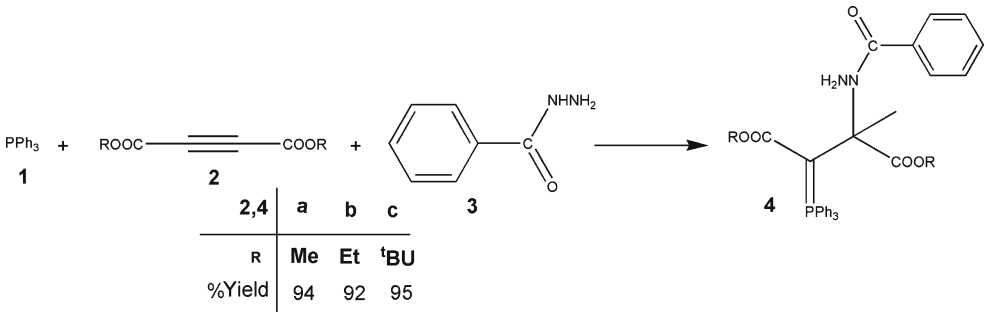

Fig. 1 The reaction between triphenylphosphine 1, dialkyl acatylenedicarboxylate 2 (2**a** 2**b** or 2**c**) and benzhydrazide 3 for generation of stable phosphorus ylides 4(4**a** 4**b** or 4**c**)

used therapeutically, including isoniazid [INH (isonicotinic hydrazide) tuberculosis antibiotic], iproniazid (tranquilizer), isocarboxazid, mebanazine, phenelzine (monoamine oxidase inhibitors), hydralazine (antihypertensive) and PHZ (phenylhydrazine; control of polycythemia vera). However, many of these compounds are no longer in use as drugs due to the severe side effects resulting from their bioactivation, which include haemolysis, liver damage, lupus erythematosus and base-pair mutation [27, 28]. Hydrazines and hydrazides are metabolically activated inhibitors. Following enzymic activation, metabolically activated inhibitors are released from the active site and can rebind the same enzyme or a different biomolecule, thereby leading to inactivation [29]. Their unwanted side effects may be due to low specificity of either the prodrug or the activated form, resulting in activation by, or inactivation of, non-target enzymes. Specificity depends on both the binding affinity and the reactivity of the activated inhibitor. The side effects observed for INH serve to illustrate the problems associated with the use of metabolically activated hydrazides as drugs. An investigation of the structural factors that control the efficiency of peroxidase inhibition by arylhydrazides is clearly necessary to assess their potential as therapeutic agents or as tools to define the activities of specific peroxidases in vivo.

Experimental

Material, methods and apparatuses used

Melting points, IR and UV spectra of all compounds were measured on an Electrothermal 9100 apparatus, a Shimadzu IR-460 spectrometer and a Cary UV/VIS spectrophotometer model Bio-300 with a 10 mm light-path quartz spectrophotometer cell, respectively. Also, the ^{1}H, ^{13}C, and ^{31}P NMR spectra were recorded on a BRUKER DRX-300 AVANCE instrument with $CDCl_3$ as solvent at 300.1, 121.4, and 75.5 MHz, respectively. In addition, the mass spectra were recorded on a Shimadzu QP 1100 EX mass spectrometer operating at an ionization potential of 70 eV. Elemental analysis for C, H and N were performed using a Heraeus CHM-O-Rapid analyzer. Dialkyl acetylenedicarboxylates, triphenlphosphine, and benzhydrazide were purchased from Fluka, (Buchs, Switzerland) and used without further purification.

Syntheses

The reaction between benzhydrazide 3 and dialkyl acetylenedicarboxylates 2 (2a, 2b or 2c) in the presence of triphenylphosphine 1 were carried out in acetone solvent at room temperature and completed within a few hours (see Fig.1).

The ^{1}H and ^{13}C NMR spectra of the crude product clearly indicated the formation of stable phosphorus ylides 4. No products other than 4 could be detected by NMR spectroscopy. The ylides moiety of these compounds is strongly conjugated with the adjacent carbonyl group and rotation around the partial double bond in (E)-4 and (Z)-4 geometrical isomers is slow on the NMR timescale at ambient temperature (see Fig. 2). Selected ^{1}H, ^{13}C, and ^{31}P NMR chemical shifts and coupling constants in the major (M) and minor (m) geometrical isomers of compounds 4a and 4b are shown in Table 1. As can be seen, only one geometrical isomer was observed for 4c, presumably, because of the bulky tert-butyl groups.

The ^{1}H NMR spectra (300 MHz) of compound 4a displayed four sharp lines at (δ=3.24, 3.76 , 3.74 and 3.81) arising from methoxy protons along with signals for methine protons at δ=5.34 and 5.26 PPm, which appear as two doublet for the N-CH group, respectively, in the major

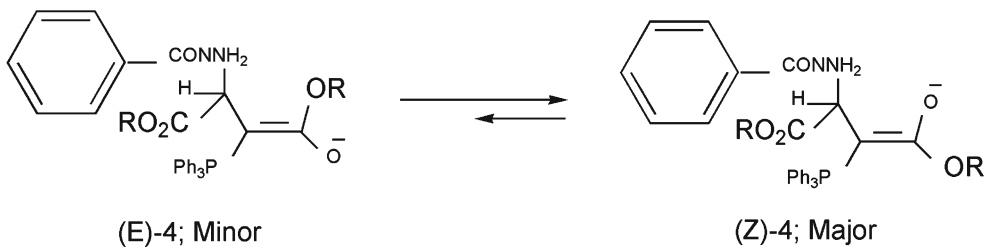

Fig. 2 Two geometrical isomers (Major and Minor) of stable phosphorus ylides 4 (4**a** or 4**b**)

Table 1 Selected ^{1}H, ^{13}C, and ^{31}P NMR chemical shifts (δ in ppm) and coupling constants (J in Hz) for H-2, OR, CO_2R, C-2, and C-3, for the two major (M) and minor (m) geometrical isomers of compounds 4a-c

		^{1}H NMR spectroscopy data				^{13}C NMR data	
Compound	Isomer (%)	H-2 ($^{3}J_{PH}$)	OR	CO_2R	C-2 ($^{2}J_{PC}$)	C-3 ($^{1}J_{PC}$)	^{31}P NMR
4a	M(68)	3.62 (br)	3.11	3.77	63.16 (15.0)	41.62 (127.0)	23.27
4a	m(32)	3.62 (br)	3.56	3.72	62.71 (15.6)	42.60 (136.3)	23.95
4b	M(65)	3.56 (br)	0.44	1.26	62.59 (15.2)	41.53 (127.1)	23.58
4b	m(35)	3.50 (br)	1.20	1.30	62.74 (15.2)	42.60 (135.2)	24.81
4c	M	3.39 (16.7)	0.86	1.53	62.64(15.7)	41.33 (127.9)	23.20

and minor geometrical isomers. The ^{13}C NMR spectrum of 4a exhibited 44 distinct resonances that are in agreement with the mixture of the two rotational isomers. Although the presence of the ^{31}P nucleus complicates both the ^{1}H and ^{13}C NMR spectra of 4a, it helps in assignment of the signals by long-range couplings with the ^{1}H and ^{13}C nuclei (see experimental section). The structural assignments made on the basis of the ^{1}H and ^{13}C NMR spectra of compounds (4a-c) were supported by the IR spectra. The carbonyl region of the spectra exhibited two distinct absorption bands for each compound (see experimental section).

On the basis of the well established chemistry of trivalent phosphorus nucleophiles [2–29], it is reasonable to assume that phosphorus ylide 4 results from the initial addition of triphenylphosphine 1 to the dialkyl acetylendicarboxylate 2 (rate constant k_2) and subsequent protonation of the 1:1 adduct (I_1) by the NH-acid 3 (rate constant k_3) to form phosphoranes 4 (rate constant k_4) (see Fig. 3).

Results and discussion

General procedure preparation of dimethyl 2-(benzhydrazide -1-yl)-3-(triphenylphosphoranylidene)-butanedioate (4a)

To a magnetically stirred solution of triphenylphosphine (0.26 g or 1 mmol) and benzhydrazide (0.33 g or 1 mmol) in 10 mL of ethyl acetate was added, dropwise, a mixture of dimethyl acetylenedicarboxylate (0.14 g or 1 mmol) in 4 mL of ethyl acetate at -5 °C over 10 min. After a few minutes stirring at room temperature, the product was filtered and recrystallized from ethyl acetate.

Table 2 The values of overall second order rate constant for the reaction between compounds 1, 2c and 3 in the presence of solvents such as, ethyl acetate and 1,2-dichloroethane respectively at all temperatures investigated

Solvent	ε	k_2. $M^{-1}.min^{-1}$			
		12.0 °C	17.0 °C	22.0 °C	27.0 °C
Ethyl acetate	6	61.5	81.5	99.5	116.9
1,2-dichloroethane	10	85.5	109.9	134.2	146.9

Colorless crystal, yield: 0.51 g, (94 %). Mp=130-132 °C, IR (KBr) (ν_{max}, cm^{-1}): 3325 and 3302 (NH_2), 1725 (C=O). MS (*m/z*, %): 540 (M^+, 1), 333 (100), 262 (20), 183 (68), 147 (51), 105 (87), 77 (76).

Major isomer (*Z*)-**4a** (66 %): ^{1}H NMR (500.1 MHz, $CDCl_3$): 3.11 and 3.77 (6 H, 2 s, 2×O*CH*$_3$), 3.62 (1 H, br, P=C-C*H*), 7.32-7.62 (20 H, m, Ar), 8.49 (2 H, br, NH_2). ^{13}C NMR (125.8 MHz, $CDCl_3$): 41.62 (d, $^{1}J_{PC}$=127.0 Hz, P=*C*), 49.22 and 52.25 (2 s, 2×O*C*H$_3$), 63.16 (d, $^{2}J_{PC}$=15.0 Hz, P=C-*C*H), 126.64 (d, $^{1}J_{PC}$=92.0 Hz, C_{ipso}), 126.91 and 128.43 (2 s, 2×C, $C_7H_8N_2O$), 128.72 (d, $^{3}J_{PC}$=12.3 Hz, C_{meta}), 131.17 (s, $C_7H_8N_2O$), 132.08 (s, C_{para}), 133.76 (s, $C_7H_8N_2O$), 133.77 (d, $^{2}J_{PC}$=9.7 Hz, C_{ortho}), 165.31 (s, $C_7H_8N_2O$), 170.32 (d, $^{2}J_{PC}$=13.2 Hz, P-C=*C*), 175.00 (d, $^{3}J_{PC}$=13.9 Hz, C=O). ^{31}P NMR (202.4 MHz, $CDCl_3$): 23.27 (Ph_3P^+-C).

Minor isomer (*E*)-**4a** (34 %): ^{1}H NMR (500.1 MHz, $CDCl_3$): 3.56 and 3.72 (6 H, 2 s, 2×O*CH*$_3$), 3.62 (1 H, br, d, P=C-C*H*), 7.32-7.62 (20 H, m, Ar), 8.15 (2 H, br, NH_2). ^{13}C NMR (125.8 MHz, $CDCl_3$): 3.11 and 3.77 (6 H, 2 s, 2×O*CH*$_3$), 3.62 (1 H, br, P=C-C*H*), 7.32-7.62 (20 H, m, Ar), 8.49 (2 H, br, NH_2). ^{13}C NMR (75.4 MHz, $CDCl_3$): 42.60 (d, $^{1}J_{PC}$=136.27 Hz, P=*C*), 50.34 and 52.06 (2 s, 2×O*C*H$_3$), 62.71 (d, $^{2}J_{PC}$=15.6 Hz, P=C-*C*H), 126.19 (d, $^{1}J_{PC}$=92.0 Hz, C_{ipso}), 126.65 and 128.53 (2 s, 2×C, $C_7H_8N_2O$), 128.72 (d, $^{3}J_{PC}$=12.3 Hz, C_{meta}), 131.37 (s, $C_7H_8N_2O$), 132.08 (s, C_{para}), 133.41 (s, $C_7H_8N_2O$), 133.77 (d, $^{2}J_{PC}$=9.7 Hz, C_{ortho}), 165.31 (s, $C_7H_8N_2O$), 170.45 (d, $^{2}J_{PC}$=12.6 Hz, P-C=*C*), 175.03 (d, $^{3}J_{PC}$=13.3 Hz, C=O).. ^{31}P NMR (202.4 MHz, $CDCl_3$): 23.95 (Ph_3P^+-C).

Diethyl 2-(1-benzoylhydrazinyl)-3-(triphenylphosphoranylidene) butanedioate (4b)

Colorless crystal, yield: 0.51 g, (90 %). Mp=128-130 °C, IR (KBr) (ν_{max}, cm^{-1}): 3423 and 3352 (NH_2), 1720 (C=O). MS (*m/z*, %): 568 (M^+, 43), 347 (10), 303 (16), 262 (29), 183 (47), 147 (26), 105 (100), 77 (70).

Major isomer (*Z*)-**4b** (65 %): ^{1}H NMR (500.1 MHz, $CDCl_3$): 0.44 (3 H, t, $^{3}J_{HH}$=7.0 Hz, OCH$_2$C*H*$_3$), 1.26 (3 H, t, $^{3}J_{HH}$=7.0 Hz, OCH$_2$C*H*$_3$), 3.56 (1 H, br, P=C-C*H*), 3.68-3.75 (2 H, m, ABX_3 system, OC*H*$_2$CH$_3$), 4.14-4.20 (2 H, m, ABX_3 system, OC*H*$_2$CH$_3$), 7.39-7.84 (20 H, m, Ar), 8.24 (2 H, br, NH_2). ^{13}C NMR (125.8 MHz, $CDCl_3$): 13.96 and 14.27 (2 s,

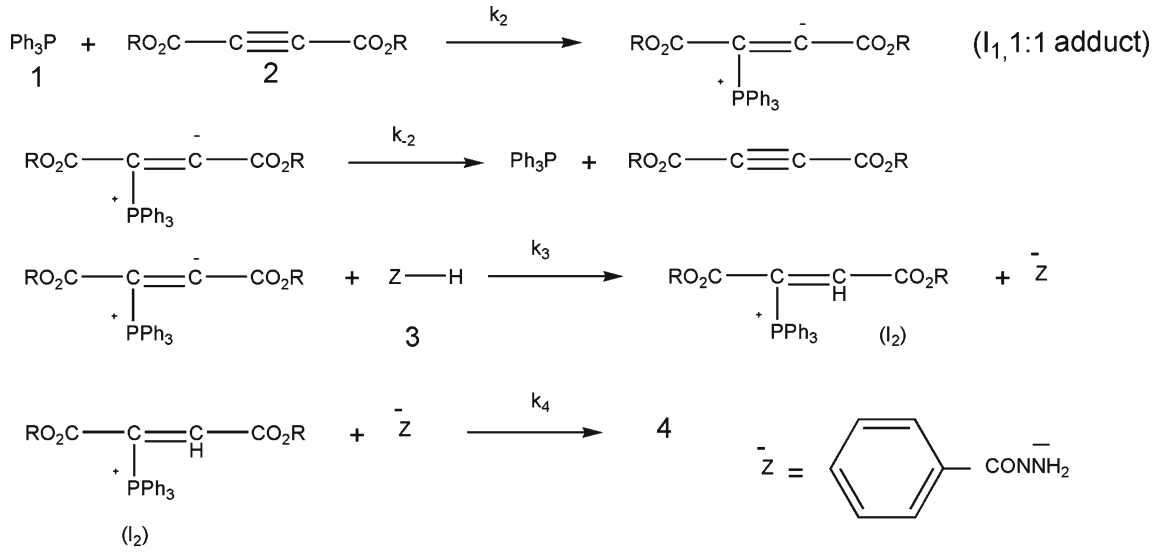

Fig. 3 Speculative proposed mechanism for the reaction between 1, 2 (2**a** 2**b** or 2**c**) and 3 on the basis of literatures [2–12] for generation of phosohorus ylides 4 (4**a** 4**b** or 4**c**) in accord with experimental studies

2×OCH_2CH_3), 41.53 (d, $^1J_{PC}$=127.1 Hz, P=*C*), 57.76 and 60.91 (2 s, 2×OCH_2CH_3), 62.59 (d, $^2J_{PC}$=15.2 Hz, P=C-*C*H), 126.82 (d, $^1J_{PC}$=92.0 Hz, C_{ipso}), 126.98, 128.36 (2 s, 2×C, $C_7H_8N_2O$), 128.58 (d, $^3J_{PC}$=8.2 Hz, C_{meta}), 131.75 and 132.02 (2 s, 2×C, $C_7H_8N_2O$), 132.71 (s, C_{para}), 133.89 (d, $^2J_{PC}$=9.8 Hz, C_{ortho}), 162.28 (s, $C_7H_8N_2O$) 170.04 (d, $^2J_{PC}$= 12.6 Hz, P-C=*C*), 174.61 (d, $^3J_{PC}$=11.0 Hz, C=O). ^{31}P NMR (202.4 MHz, $CDCl_3$): 23.58 (Ph_3P^+-C).

Minor isomer (*E*)-**4b** (35 %): ^{1}H NMR (500.1 MHz, $CDCl_3$): 1.20 (3 H, t, $^3J_{HH}$=7.0 Hz, OCH_2CH_3), 1.30 (3 H, t, $^3J_{HH}$=7.0 Hz, OCH_2CH_3), 3.50 (1 H, br, P=C-C*H*), 3.66-3.73 (2 H, m, ABX_3 system, OCH_2CH_3), 4.11-4.22 (2 H, m, ABX_3 system, OCH_2CH_3), 7.39-7.84 (20 H, m, Ar), 8.14 (2 H, br, NH_2). ^{13}C NMR (125.8 MHz, $CDCl_3$): 14.17 and 14.33 (2 s, 2× OCH_2CH_3), 42.60 (d, $^1J_{PC}$=135.2 Hz, P=*C*), 58.28 and 61.28 (2 s, 2×OCH_2CH_3), 62.74 (d, $^2J_{PC}$=15.2 Hz, P=C-*C*H), 126.45 (d, $^1J_{PC}$=92.0 Hz, C_{ipso}), 127.87 and 128.81 (2 s, 2×C, $C_7H_8N_2O$), 128.58 (d, $^3J_{PC}$=8.2 Hz, C_{meta}), 131.88 and 132.15 (2 s, 2×C, $C_7H_8N_2O$), 132.71 (s, C_{para}), 132.71 (s, C_{para}), 133.89 (d, $^2J_{PC}$=9.8 Hz, C_{ortho}), 164.95 (s, $C_7H_8N_2O$) 170.15 (d, $^2J_{PC}$=12.6 Hz, P-C=*C*), 174.36 (d, $^3J_{PC}$=11.0 Hz, C=O).. ^{31}P NMR (202.4 MHz, $CDCl_3$): 24.81 (Ph_3P^+-C).

Di-tert-butyl 2-(1-benzoylhydrazinyl)-3-(triphenylphosphoranylidene) butanedioate (3c)

Colorless crystal, yield: 0.60 g, (96 %). Mp=113-115 °C, IR (KBr) (ν_{max}, cm^{-1}): 3342 and 3287 (NH_2), 1729 (C=O). MS (*m/z*, %): 624 (M^+, 40), 376 (5), 319 (34), 262 (85), 183 (31), 147 (66), 105 (100), 77 (79), 57 (91).

(***Only rotamer***) (*Z*)-**4c**: ^{1}H NMR (500.1 MHz, $CDCl_3$): 0.86 and 1.53 (18 H, 2 s, 2×$OCMe_3$), 3.39 (1 H, d, $^3J_{PH}$= 16.7 Hz, P=C-C*H*), 7.39-7.84 (m, 20 H, Ar), 8.11 (br, 2 H, NH_2). ^{13}C NMR (125.8 MHz, $CDCl_3$): 27.95 and 28.26 (2× $OCMe_3$), 41.33 (d, $^1J_{PC}$=127.9 Hz, P=*C*-CH), 62.64 (d, $^2J_{PC}$=15.7 Hz, P=C-*C*H), 77.28 and 80.67 (2×$OCMe_3$), 126.98 (s, $C_{37}H_{41}N_2O_5$), 127.26 (d, $^1J_{PC}$=91.9 Hz, C_{ipso}),

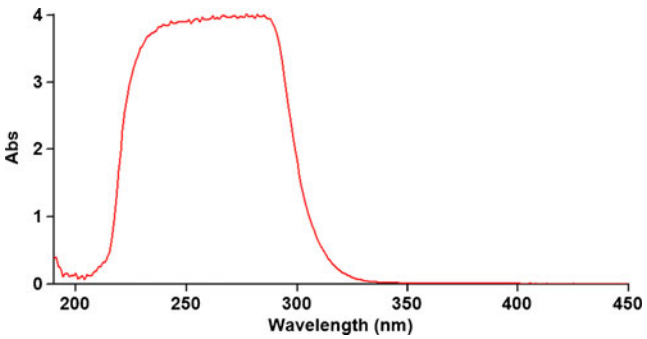

Fig. 4 The UV spectrum of 10^{-3} M triphenylphosphine 1 in 1, 2-dichloroethane

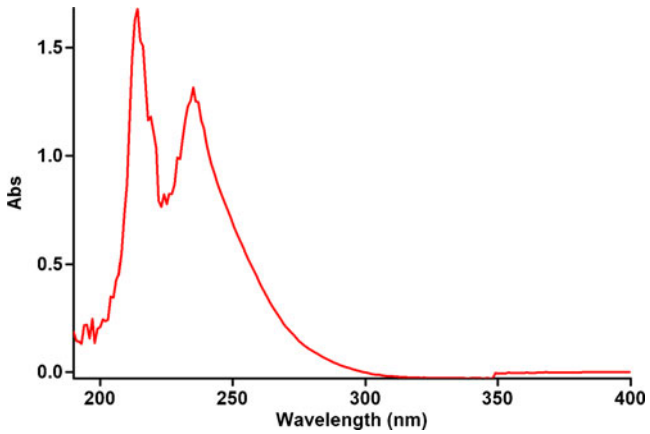

Fig. 5 The UV spectrum of 10^{-3} M di-tert-butyl acetylenedicarboxylate 2c in 1, 2-dichloroethane

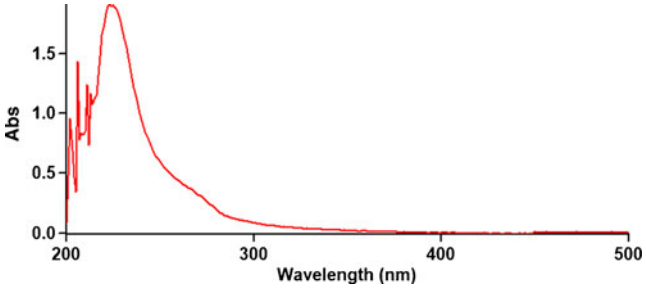

Fig. 6 The UV spectrum of 10^{-3} M benzhydrazide 3 in 1, 2-dichloroethan

128.28 (s, $C_{37}H_{41}N_2O_5$), 128.54 (d, $^3J_{PC}$=8.3 Hz, C_{meta}), 131.75 and 132.54 (s, $C_{37}H_{41}N_2O_5$), 132.78 (s, C_{para}), 133.89 (d, $^2J_{PC}$=9.8 Hz, C_{ortho}), 168.43 (s, N-C=O), 170.14 (d, $^2J_{PC}$=11.7 Hz, P-C=*C*), 174.27 (d, $^3J_{PC}$=11.9 Hz, C=O). ^{31}P NMR (202.4 MHz, $CDCl_3$): δ 23.20 (Ph_3P^+-C).

Kinetics studies

To gain further insight into the reaction mechanism between triphenylphosphin 1, dialkyl acetylenedicarboxylates (2a, 2b and 2c) and benzhydrazide 3 (as a NH- heterocyclic compound) for generation of phosphorus ylids 4a-c, a kinetic study of the reactions was undertaken by UV spectrophotometeric technique. First, it was necessary to find the appropriate wavelength to follow the kinetic study of the reaction. For this purpose, in the first experiment, 3×10^{-3} M solution of compounds 1, 2c and 3 was prepared in 1, 2-dichloroethane as solvent. An approximately 3 mL aliquot from each reactant was pipetted into a 10 mm light path quartz spectrophotometer cell, and the relevant spectra were recorded over the wavelength range 190-400 nm. Figures 4, 5 and 6 show the ultraviolet spectra of compounds 1, 2c and 3 respectively. In a second experiment, a 1 mL aliquot from the 3×10^{-3} M solutions of each compound of 1 and 3 was pipetted first into a quartz spectrophotometer cell (as there is no reaction between them), later 1 mL aliquot of the 3×10^{-3} M solution of reactant 2c was added to the mixture and the reaction monitored by recording scans of the entire spectra every 8 min over the whole reaction time at ambient temperature. The ultra-violet spectra shown in Fig. 7 are typical. From this, the appropriate wavelength was found to be 303 nm (corresponding mainly to product 4c). Since at this wavelength, compounds 1, 2c and 3 have relatively no absorbance value. This then provided the opportunity to fully investigate the kinetics of the reaction between triphenylphosphine 1, di-tert-butyl acetylenedicarboxylate 2c and benzhydrazide 3 at 330 nm in the presence of 1, 2-dichloroethaneas solvent. Since the spectrophotometer cell of the UV instrument had a 10-mm light-path cuvette, the UV-vis spectra of compound 4c were measured over the concentration range (2×10^{-4} M ≤ M_{4c} ≤10^{-3} M) to check for a linear relationship between absorbance values and concentrations. With the suitable concentration range and wavelength identified, the following procedure was employed.

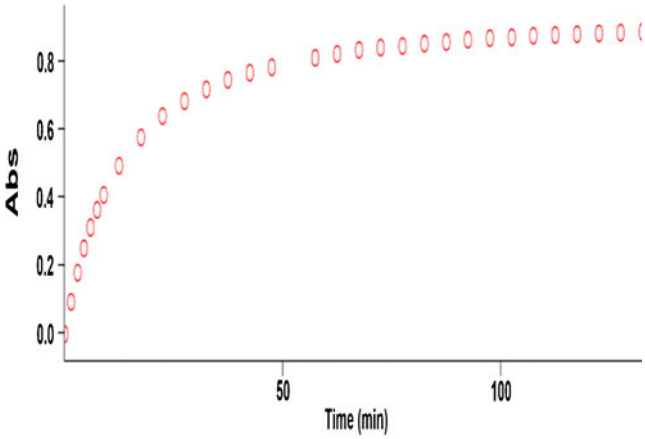

Fig. 8 The experimental absorbance changes (dotted line) against time at 330 nm for the reaction between compounds 1, 2**c** and 3 at12.0 °C in 1,2-dichloroethane

For each kinetic experiment, first a 1 mL aliquot from each freshly made 3×10^{-3} M solution of compounds 1 and 3 in 1, 2-dichloroethane was pipetted into a quartz cell, and then a 1 mL aliquot of the 3×10^{-3} M of solution of reactant 2c was added to the mixture, keeping the temperature at 12.0 °C. The reaction kinetics was followed by plotting UV absorbance against time. Figure 8 shows the absorbance change (dotted line) versus time for the 1:1:1 addition reaction between compounds 1, 2c and 3 at 12.0 °C. The infinity absorbance (A_∞)

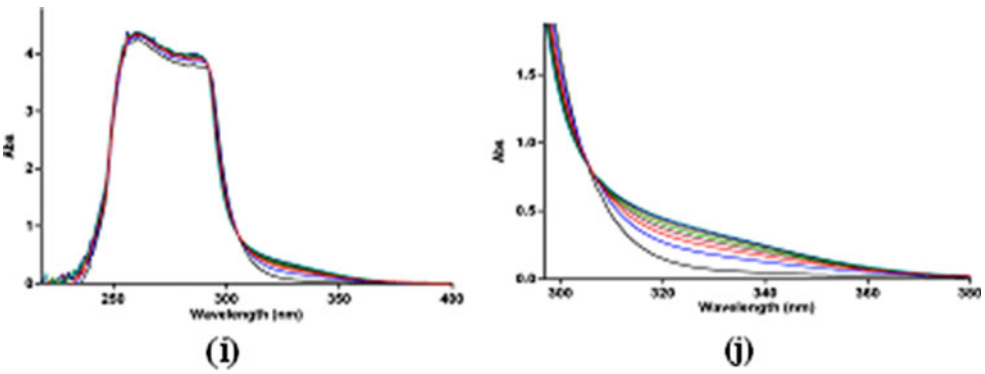

Fig. 7 **i** The UV spectra of the reaction between 1, 2c and 3 with 10^{-3} M concentration of each compound as reaction proceeds in 1, 2-dichloroethane with 10 mm light-path cell for generation of ylide 4c. **j** Expanded section of UV spectra one the wavelength range 300-380 nm

that is the absorbance at reaction completion, can be obtained from Fig. 8 at t =132 min. With respect to this value, zero, first or second curve fitting could be drawn automatically for the reaction by the software [30, 31] associated with the UV instrument. Using the original experimental absorbance versus time data provided a second-order fit curve (full line) that fits exactly the experimental curve (dotted line) as shown in Fig. 9. Thus, the reaction between triphenylphosphine 1, di-tert-butyl acetylenedicarboxylate 2c and 3 follows second-order kinetics. The second-order rate constant (k_2) is then automatically calculated using a standard equation [31] within the program at 12.0 °C. It is reported in Table 1.

Furthermore, kinetic studies were carried out using the same concentration of each reactant in the continuation of experiments with concentrations of 5×10^{-3} M and 7×10^{-3} M respectively. As expected, the second-order rate constant was independent of concentration and its value was the same as in the previous experiment. In addition, the overall order of reaction was also 2.

Effect of solvents and temperature

To determine the effect of change in temperature and solvent environment on the rate of reaction, it was elected to perform various experiments at different temperatures and solvent polarities but otherwise under the same conditions as for the previous experiment. For this purpose, ethyl acetate with six dielectric constant was chosen as a suitable solvent since it not only could dissolve all compounds but also did not react with them. The effects of solvents and temperature on the rate constant are given in Table 1. The results show that the rate of reaction in each case was increased at higher temperature. In addition, the rate of reaction between 1, 2c and 3 was accelerated in a higher dielectric constant environment (1, 2-dichloroethane) in comparison with a lower dielectric constant environment (ethyl acetate) at all temperatures investigated. In the temperature range studied, the dependence of the second-order rate constant (Ln k_2) of the reactions on reciprocal temperature is consistent with the Arrhenius equation, giving activation energy of the reaction between 1, 2c and 3 (26.0 kJ mol^{-1}) from the slope of Fig. 10.

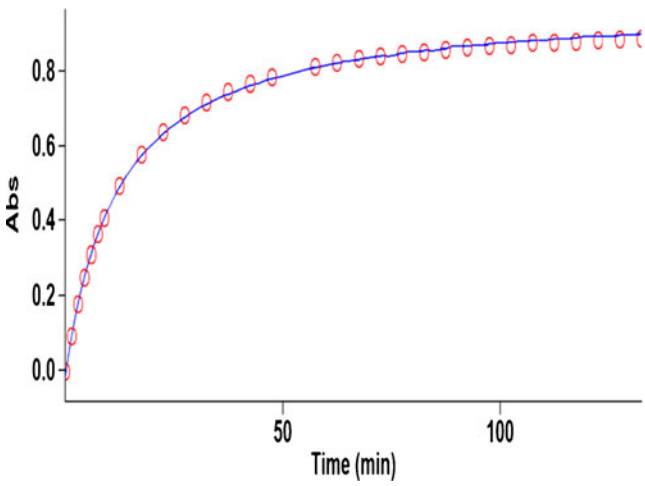

Fig. 9 Second order fit curve (full line) accompanied by the original experimental curve (dotted line) for the reaction between compounds 1, 2**c** and 3 at 330 nm and12.0 °C in 1,2-dichloroethane

Effect of concentration

To determine reaction order with respect to triphenylphosphine 1 and dialkyl acetylene-dicarboxylate 2 (2c), in the continuation of experiments, all kinetic studies were carried out in the presence of excess 3. Under this condition, the rate equation may therefore be expressed as:

$$rate = k_{obs}[1]^{a}[2]^{\beta}\ k_{obs} = k_2[3]^{\gamma}\ or\ Lnk_{obs} = Lnk_2 + \gamma Ln[3]. \quad (1)$$

In this case (3×10^{-2} M of 3 instead of 3×10^{-3} M) using the original experimental absorbance versus time data provides a second order fit curve (full line) against time at 330 nm which exactly fits the experimental curve. The value of rate constant was the same as that obtained from the previous experiment (3×10^{-3} M). Repetition of the experiments with 5×10^{-2} M and 7×10^{-2} M of 3 gave, separately, the same fit curve and rate constant. In fact, the experimental data indicated that the observed pseudo second order rate constant (k_{obs}) was equal to the second order rate constant (k_2), this is possible when γ is zero in Eq. 1. It appears, therefore, that the reaction is zero and second order with respect to 3 (NH-acid) and the sum of 1 and 2 (2c) ($\alpha + \beta = 2$), respectively.

To determine reaction order with respect to dialkyl acetylenedicarboxlated (2c), the continuation of experiment was performed in the presence of excess of 1. Under this condition, the rate equation may therefore be expressed as:

$$rate_{=}k'_{obs}[2]^{b}[3]^{\gamma},\ k'_{obs=}k_2[1]^{a}. \quad (2)$$

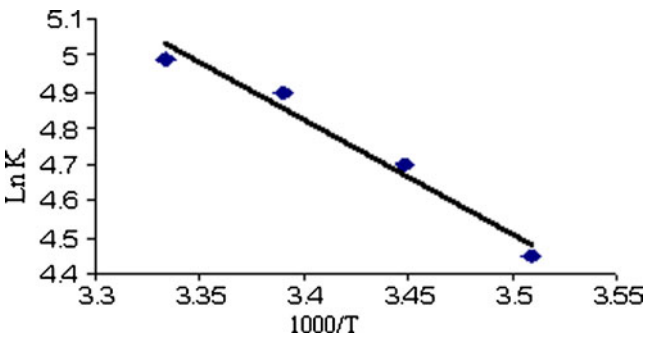

Fig. 10 Dependence of second order rate constant (Ln k_2) on reciprocal temperature for the reaction between compounds 1, 2**c** and 3 measured at wavelength 330 nm in 1,2-dichloroethane in accordance with Arrhenius equation

The original experimental absorbance versus time data provide a pseudo first order fit curve at 330 nm, which exactly fits the experimental curve (dotted line) as shown in Fig. 11.

As a result since $\gamma=0$ (as determined previously), it is reasonable to accept that the reaction is first order with respect to compound 2c ($\beta = 1$). Because the overall order of reaction is 2 ($\alpha + \beta + \gamma=2$) it is obvious that $\alpha_{=}1$ and order of triphenylphosphine must be equal to one. This observation was obtained also for reactions between (1, 2b and 3) and (1, 2a and 3). Based on the above results, a simplified proposed reaction mechanism is shown in Fig. 3.

The experimental results indicate that the third step (rate constant k_3) is possibly fast. In contrast, it may be assumed that the third step is the rate determining step for the proposed mechanism. In this case the rate law can be expressed as follows:

$$rate = k_3[I_1][3]. \tag{3}$$

The steady state assumption can be employed for $[I_1]$ which is generated by the following equation:

$$[I_1] = \frac{k_2[1][2]}{k_{-2} + k_3[3]}. \tag{4}$$

The value of $[I_1]$ can be replaced in Eq. 3 to obtain this equation:

$$rate = \frac{k_2k_3[1][2][3]}{k_{-2} + k_3[3]}. \tag{5}$$

Since it was assumed that k_3 is relevant to the rate determining step, it is reasonable to make the following assumption:

$$k_{-2} >> k_3[3]. \tag{6}$$

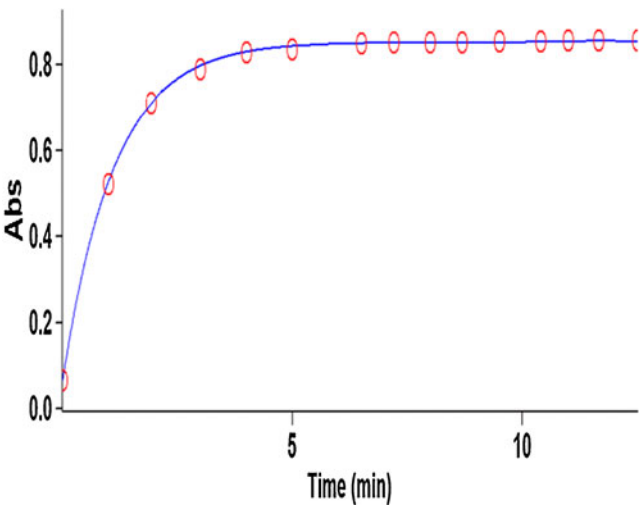

Fig. 11 Pseudo first order fit curve (full line) for the reaction between 1 and 3 in the presence of excess 1 (10^{-2} M) at 330 nm and12.0 °C in 1, 2-dichloroethane

So the rate low becomes:

$$rate = \frac{k_2k_3[1][2][3]}{k_{-2}}. \tag{7}$$

The final equation is indicates that overall order of reaction is three which is not compatible with experimental overall order of reaction (= two). In addition, according to this equation, the order of reaction with respect to benzhydrazide 3 is one, whereas it was actually shown to be equal to zero. For this reason, it appeared that the third step is fast. If we assume that the fourth step (rate constant k_4) is the rate-determining step for the proposed mechanism, on experimental study in this case, there are two ionic species to consider in the rate determining step, namely phosphonium ion (I_2) and benzhydrazide ion (Z^-). The phosphonium and benzhydrazide ions, as we see in Fig. 3, have full positive and negative charges and form very powerful ion- dipole bonds to the 1,2-dichloroethane, the high dielectric constant solvent. However, the transition state for the reaction between two ions carries a dispersed charge, which here is divided between the attacking benzhydrazide and the phosphonium ions. Bonding of solvent (1, 2-dichloroethane) to this dispersed charge would be much weaker than to the concentrated charge of benzhydrazide and phosphonium ions. The solvent thus stabilize the species ions more than it would the transition state, and therefore E_a would be higher, slowing down the reaction. However, in practice, 1, 2-dichloroethane speeds up the reaction and for this reason, the fourth step, which is independent of the change in the solvent medium, could not be the rate determining step. Furthermore, the rate law of formation of the product (fourth step) for a proposed reaction mechanism with application of steady state assumption can be expressed by:

$$rate = k_4[I_2][Z^-]. \tag{8}$$

By application of steady state for $[I_2]$ and $[Z^-]$, and replacement of their values in the above equation, the following equation is obtained:

$$rate = \frac{k_2k_3[1][2][3]}{k_{-2} + k_3[3]}. \tag{9}$$

This equation is independent of rate constant for the fourth step (k_4) and shows why the fourth step would not be affected

Table 3 Values of overall second order rate constant for the reaction between 1, 2b and 3 in the presence of solvents such as ethyl acetate and 1, 2-dichloroethane respectively at all temperatures investigated

Solvent	ε	k_2. $M^{-1}.min^{-1}$			
		12.0 °C	17.0 °C	22.0 °C	27.0 °C
Ethyl acetate	6	267.8	335.6	397.4	445.8
1,2-dichloroethane	10	735.0	812.4	897.8	1006

Table 4 The values of overall second order rate constant for the reaction between 1, 2a and 3 in the presence of solvents such as, ethyl acetate and 1, 2-dichloroethane respectively at all temperatures investigated

Solvent	ε	k_2. $M^{-1}.min^{-1}$			
		12.0 °C	17.0 °C	22.0 °C	27.0 °C
Ethyl acetate	6	348.0	429.5	473.4	547.0
1,2-dichloroethane	10	1288.9	1290.9	1360.5	1458.2

by a change in the solvent medium. In addition, it has been suggested earlier that the kinetics of ionic species phenomena (e.g., the fourth step) are very fast [32]. If the first step (rate constant k_2) were the rate determining step, in this case, two reactants (triphenylphosphine 1 and dialkyl acetylenedicarboxylate 2), as we see in Fig. 3, have no charge and could not form strong ion-dipole bonds to the high dielectric constant solvent, 1, 2-dichloroethane. However, the transition state carries a dispersed charge which here is divided between the attacking 1 and 2 and, hence, bonding of solvent to this dispersed charge is much stronger than the reactants, which lack charge. The solvent thus stabilizes the transition state more than it does the reactants and, therefore, E_a is reduced which speeds up the reaction. Our experimental results show that the solvent with higher dielectric constant exerts a powerful effect on the rate of reaction (in fact, the first step has rate constant k_2 in the proposed mechanism) but the opposite occurs with the solvent of lower dielectric constant, (see Tables 1, 3 and 4). The results of the current work (effects of solvent and concentration of compounds) have provided useful evidence for steps 1 (k_2), 3 (k_3) and 4 (k_4) of the reactions between triphenylphosphine 1, dialkyl acetylenedicarboxylate 2 (2a, 2b or 2c) and benzhydrazide 3. Two steps involving 3 and 4 are not rate-determining steps, although the discussed effects, taken altogether, are compatible with the first step (k_2) of the proposed mechanism and would allow it to be the rate-determining step in our experimental study. However, a good kinetic description of the experimental result using a mechanistic scheme based upon the steady state approximation is frequently taken as evidence of its validity. By application of this, the rate formation of product 4 from the reaction mechanism (Fig. 3) is given by:

Table 5 The activation parameters involving $\Delta G^{\#}$, $\Delta S^{\#}$ and $\Delta H^{\#}$ for the reactions between 1, 2a and 3, 1, 2b and 3 and also 1, 2c and 3 at 12.0 °C in 1, 2-dicholoroethane

Reactions	$\Delta G^{\#}$(kJ.mol^{-1})	$\Delta H^{\#}$(kJ.mol^{-1})	$\Delta S^{\#}$(J.mol^{-1}.K^{-1})
1, 2a and 3	102.46	9.26	-326.87
1, 2b and 3	103.27	11.86	-320.58
1, 2c and 3	106.60	36.76	-244.95

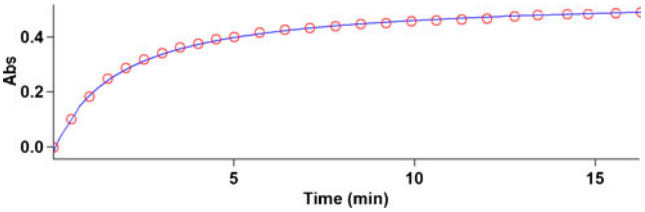

Fig. 12 Second order fit curve (full line) accompanied by the original experimental curve (dotted line) for the reaction between compounds 1, 2**b** and 3 at 330 nm and 12.0 °C in 1,2-dichloroethane

$$\frac{d[4]}{dt} = \frac{d[ylide]}{dt} = rate = k_4[I_2][Z^-]. \quad (10)$$

We can apply the steady-state approximation to $[I_1]$ and $[I_2]$;

$$\frac{d[I_1]}{dt} = k_2[1][2] - k_{-2}[I_1] - k_3[I_1][3] \quad (11)$$

$$\frac{d[I_2]}{dt} = k_3[I_1][3] - k_{-4}[I_2] - k_4[I_2][Z^-].$$

To obtain a suitable expression for $[I_2]$ to put into Eq. 10 we can assume that, after an initial brief period, the concentration of $[I_1]$ and $[I_2]$ achieve a steady state with their rates of formation and rates of disappearance just balanced. Therefore $\frac{d[I_1]}{dt}$ and $\frac{d[I_2]}{dt}$ are zero and we can obtain expressions for $[I_2]$ and $[I_1]$ as follows:

$$\frac{d[I_2]}{dt} = 0, \quad [I_2] = \frac{k_3[I_1][3]}{k_4[Z^-]} \quad (12)$$

$$\frac{d[I_1]}{dt} = 0, \quad [I_1] = \frac{k_2[1][2]}{k_{-2} + k_3[3]}. \quad (13)$$

We can now replace $[I_1]$ in Eq. 12 to obtain this equation:

$$[I_2] = \frac{k_2k_3[1][2][3]}{k_4[Z^-][k_{-2} + k_3[3]]}. \quad (14)$$

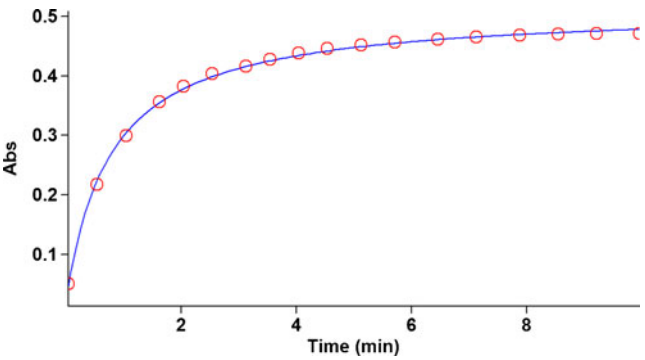

Fig. 13 Second order fit curve (full line) accompanied by the original experimental curve (dotted line) for the reaction between compounds 1, 2**a** and 3 at 330 nm and 12.0 °C in 1,2-dichloroethane

The value of $[I_2]$ can be put into Eq. 10 to obtain the rate Eq. 15 for proposed mechanism:

$$rate = \frac{k_2 k_3 k_4 [1][2][3][Z^-]}{k_4[N^-][k_{-2} + k_3[3]]} \quad or$$
$$rate = \frac{k_2 k_3 [1][2][3]}{[k_{-2} + k_3[3]]}. \tag{15}$$

Since experimental data indicated that steps 3 (k_3) and 4 (k_4) are fast but step 1 (k_2) is slow, it is therefore reasonable to make the following assumption:

$$k_3[3] >> k_{-2}. \tag{16}$$

So the rate equation becomes:

$$rate = k_2[1][2]. \tag{17}$$

This equation which was obtained from a mechanistic scheme (shown in Fig. 3) by applying the steady-state approximation is compatible with the results obtained by UV spectrophotometery. With respect to the Eq. 17 that is overall reaction rate (Fig. 1), the activation parameters involving $\Delta G^{\#}$, $\Delta S^{\#}$ and $\Delta H^{\#}$ could be now calculated for the first step (rate determining step), as an elementary reaction, on the basis of Eyring equation. The results are reported in Table 5.

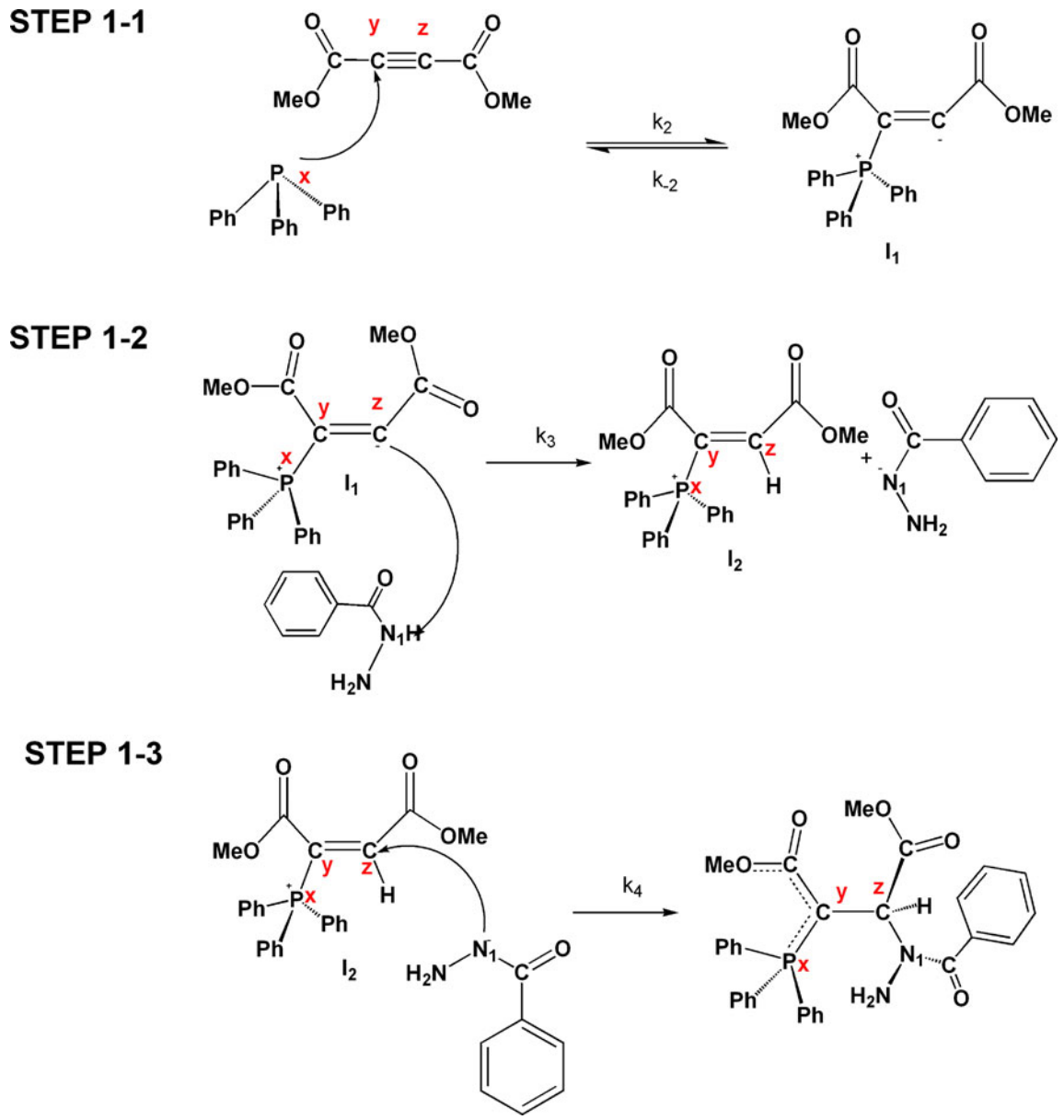

Fig. 14 Speculative proposed mechanism 1 involving three steps for generation of ylide 4

Further kinetic investigations

Effect of structure of dialkyl acetylenedicarboxylates

To confirm the above observations, further experiments were performed with diethyl acetylenedicarboxylate 2b and dimethyl acetylenedicarboxylate 2a, respectively, under the same conditions used in the previous experiments. The values of the second-order rate constant (k_2) for the reactions between (1, 2b and 3) and (1, 2a and 3) are reported in Tables 3 and 4, respectively for all solvents and temperatures investigated. The original experimental absorbance curves (dotted line) accompanied by the second order fit curves (full line), which exactly fit experimental curves (dotted line) (Figs. 12 and 13) confirm the previous observations again for both reactions at 12.0 °C and 330 nm.

As can be seen from Tables 3 and 4 the behavior of diethyl acetylenedicarboxylate 2b and dimethyl acetylenedicarboxylate 2a is the same as for the di-tert-butyl acetylenedicarboxylate 2c (Table 1) with respect to the reaction with triphenylphosphine 1 and benzhydrazide 3. The rate of the former reactions was also accelerated in a higher dielectric constant environment and with higher temperatures; however, these rates of the former reactions under the same condition (12.0 °C) are approximately 14.00 to 9.00 times more than for the reaction with di-tert-butyl acetylenedicarboxylate 2c (see Tables 1, 3 and 4). It seems that both inductive and steric factors for the bulky alkyl groups in 2c tend to reduce the overall reaction rate (see Eq. 17). In the case of dimetyl acetylenedicarboxylate 2a, the lower steric and inductive effects of the dimethyl groups exert a powerful effect on the rate of reaction.

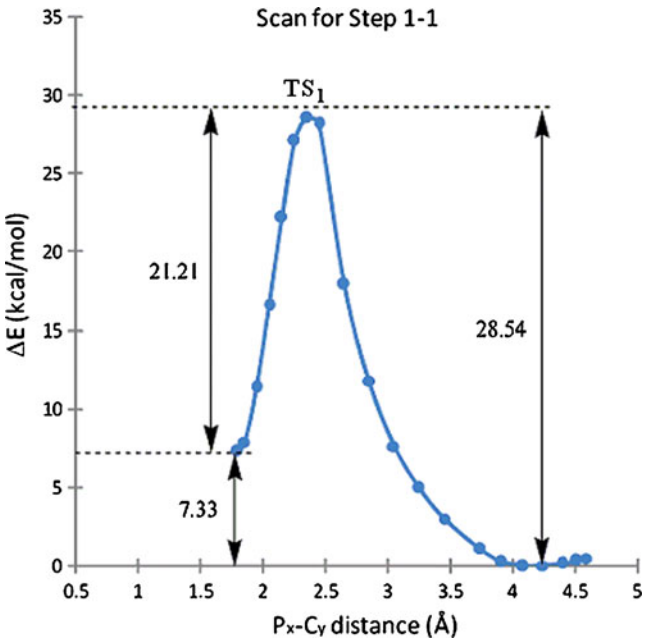

Fig. 15 The potential energy profile of the $step_{1\text{-}1}$ in mechanism 1 at HF/6-31 G(d,p) [33] level with extra 6-31 + G(3df,3pd) basis set for P atom

Table 6 The first stretching frequency for all species in mechanism 1 at HF/6-31 G(d,p) level of theory

Species	First stretching frequency
dimethyl acetylenedicarboxylate (DMAD)	30.88
Triphenylphosphine (TPP)	29.78
N-H acids benzohydrazide	64.41
ylide 4	13.23
intermediate I_1	16.14
intermediate I_2	18.03
TS_1	-218.08
TS_2	-1515.82

Theoretical kinetic studies

A typical organic reaction proceeds in a special mechanism. There may be many proposed mechanisms for a typical organic reaction. Experimental methods have many instrumental limitations such as trapping the intermediates or transition states (TSs) in confirming the mechanism that reactions proceeded from it. Computational methods can make confirming the mechanism eases cheaper and exacter. For this reaction, three speculative mechanisms were theoretically investigated for the reaction between triphenylphosphine (TPP), dimethyl acetylenedicarboxylate in the presence of N-H acid such as benzhydrazide in the gas phase in order to confirm a better understanding of a desired

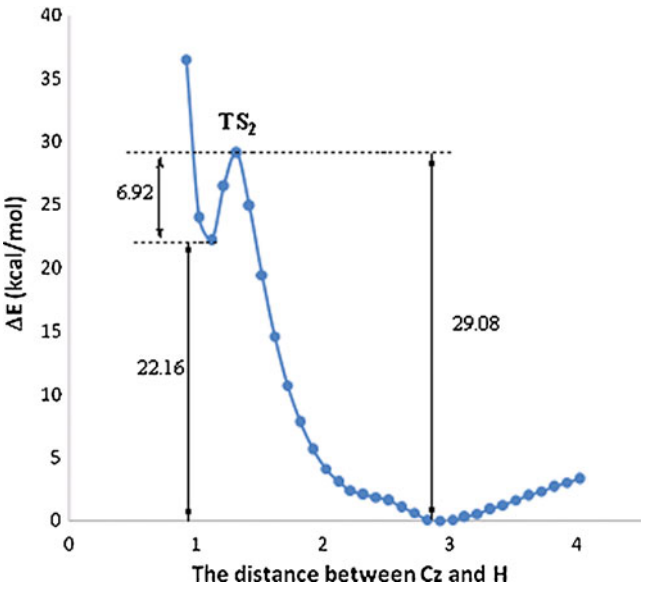

Fig. 16 Energy profile for second step of mechanism 1 at HF/6-31 G (d,p) [33] with extra 6-31 + G(3df,3pd) basis set for P atom. When the H atom of bezohydrazide is gradually brought near to the carbanion (C_z) of intermediate I for generation of intermediate 2

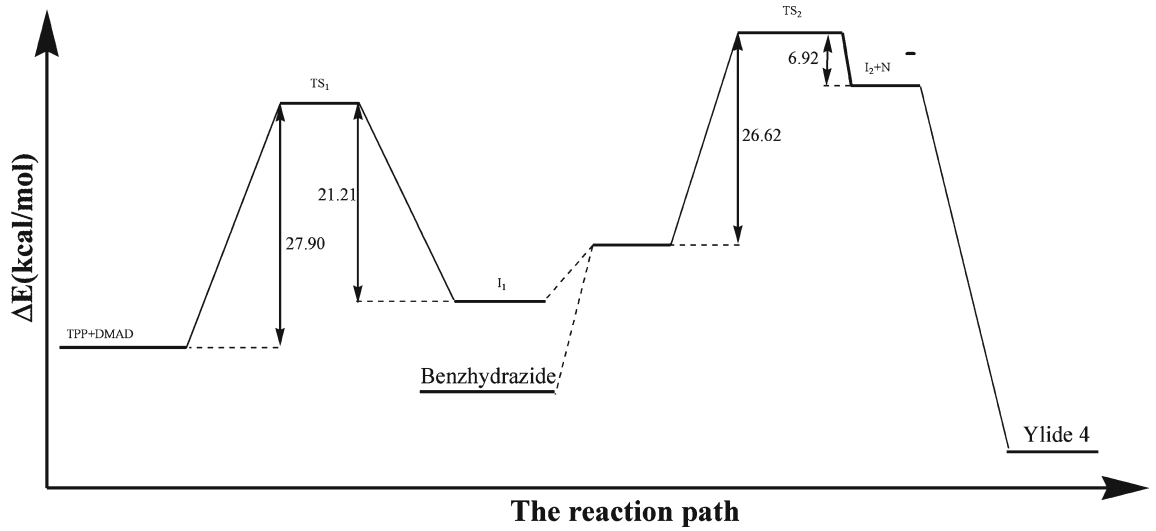

Fig. 17 The total potential surface of title reaction on the basis of speculative mechanism 1 at the HF/6-31 G(d,p) level of theory

mechanism in comparison with the speculative experimental mechanism.

Computational methods

The geometries of the reactions, products, intermediate (I) and transition states (TS) involved in the reaction were optimized at the HF/6-31 G(d,p) [33, 34] (with extra 6-31+G(3df,3pd) basis set for P atom) level of theory. Harmonic vibrational frequencies were obtained for the verification of the optimized geometries at HF/6-31 G(d,p) with extra bases set at HF/6-31 +G(3df,3pd) for phosphorus atom. Transition states were characterized by one imaginary vibrational frequency. A higher level of electronic correlation method, B3LYP/6-311 ++G(d,p) [35, 36], is employed in the single-point energy calculation to improve the accuracy of energetic information on the minimum energy path (MEP). All calculations were performed with the GAMESS program [37].

Theoretical investigations for the speculative proposed mechanism 1

Speculative theoretical proposed mechanism 1 is the same, in a joint experimental proposed mechanism (Fig. 3) and shown in Fig. 14. In the first $step_{1\text{-}1}$ of mechanism 1 (Fig. 14), the concerted reaction is initiated with C_y-C_z bond cleavage and P_x-C_y bond formation. The first transition state ($TS_{1\text{-}1}$, see Fig. 15) has a breaking C_y-C_z bond distance of 1.24 angstrom and a forming P_x-C_y bond distance of 2.31 angstrom. The calculated vibration frequencies at HF/6-31 G(d,p) level which have been listed in Table 6 show that TPP, dimethy acetylendicarboxylate (DMAD) and dipolar phosphonium ion (I_1) are true minimum points.

It should be noted here that TS_1 optimized at HF/6-31 G (d,p) level and calculated imaginary frequency (218i) implies that $TS_{1\text{-}4}$ is a transition state.

In the second $step_{1\text{-}2}$ of mechanism 1, the concerted reaction occurs with the C_z-H bond formation between dipole phosphonium ion (I_1) and benzhydrazide for generation of another intermediate namely phosphonium (I_2). The second transition state ($TS_{1\text{-}2}$, see Fig. 16) has a forming C_z-H bond distance of 1.29 angstrom. Herein, $TS_{1\text{-}2}$ showed one imaginary frequency at 1516i cm^{-1} (see Table 6).

In the third $step_{1\text{-}3}$ of mechanism 1 (k_4), the concerted reaction is started between two species ions namely phosphonium ion (I_2) and benzhydrazide ion for generating ylide 4. In this step, we could not find any TS in spite of numerous attempts due to the kinetics of ionic species phenomena are very fast, Herein, two species ions (phosphonium and benzhydrazideions) participate to generate the ylide 4. Activation energy for the each step of mechanism 1 is 27.90 (k_2), 26.62 (k_3) and 0.0 (k_4) kcal mol^{-1}, respectively. For the title reaction the total potential energy profile is shown in Fig. 17.

Activation parameters involving $\Delta G^{\neq}$, $\Delta H^{\neq}$ and $\Delta S^{\neq}$ were calculated for each step of mechanism 1[fn1] that is shown in Table 7.

Subsequently, rate constants and activation energy were obtained from the Eyring equation[fn2] that is accumulated in Table 8.

Table 7 The activation parameters involving $\Delta G^{\neq}$, $\Delta S^{\neq}$and $\Delta H^{\neq}$ for each step of mechanism 1

$\Delta G_I^{\#}$	1.277×310^5	$\Delta H_I^{\#}$	7.589×10^4	$\Delta S_I^{\#}$	1.736×10^2
$\Delta G_{III}^{\#}$	1.265×10^5	$\Delta H_{III}^{\#}$	5.113×10^4	$\Delta S_{III}^{\#}$	-2.527×10^2
$\Delta G_{IV}^{\#}$	-1.952×10^5	$\Delta H_{IV}^{\#}$	-5.333×10^5	$\Delta S_{IV}^{\#}$	-1.134×10^1
$\Delta G_{total}^{\#}$	-4.233×10^4	$\Delta H_{total}^{\#}$	-1.701×10^5	$\Delta S_{total}^{\#}$	-4.284×10^2

Table 8 The rate contestant (k) and activation energy for each step of mechanism 1

Rate contestant J .mol^{-1}	Activation energy J .mol^{-1}	Steps of mechanism 1
$k_2=0.67\times10^{-6}$	$Ea_2=7.8\times10^{4}$	1
$k_{-2}=2.05\times10^{-6}$	$Ea_{-2}=0.11\times10^{4}$	2
$k_3=1.08\times10^{-6}$	$Ea_3=5.4\times10^{4}$	3

Theoretical investigations for the speculative proposed mechanism 2

The first step of speculative mechanisms 1 and 2 is the same. In the second step$_{2\text{-}2}$ (shown in Fig. 18, step$_{2\text{-}2}$), the concerted reaction is initiated with N_1-H bond cleavage and the two H-O_w and N_1-C_z bonds formation while passing through a second transition state ($TS_{2\text{-}2}$) on the basis of five-member ring geometry for generation of intermediate 2 (I_2).

The transition state ($TS_{2\text{-}2}$) has a breaking N_1-H distance of 1.07 angstrom, a forming H-O_w bond distance of 1.53 and a forming N_1-C_z bond distance of 1.50 angstrom for generation of intermediate I_2. Imaginary frequency (1740i) implies that $TS_{2\text{-}2}$ is a transition state.

In the third step of mechanism 2, intermediate I_2 is converted to the phosphorus ylide 4 while passing through a third transition state ($TS_{2\text{-}3}$) containing four-member ring. Imaginary frequency (1345i) implies that $TS_{2\text{-}3}$ is a transition state. Herein, concerted reaction is preceded with C_z-C double bond and O_w-H single bond cleavage along with the two C-O_w double bond and C_z-H single bond formation. Activation energy for the steps of mechanism 2 involving first $TS_{2\text{-}1}$(=$TS_{1\text{-}1}$), second $TS_{2\text{-}2}$ and third $TS_{2\text{-}3}$ were obtained according to the same calculations that have been employed for mechanism 1. They are 27.90 (k_2), 19.59 (k_3) and 60.27 (k_4) kcal mol^{-1}, respectively.

Theoretical investigation for the speculative proposed mechanism 3

The first step of mechanism 3 (step $_{3\text{-}1}$) is the same as the first steps of mechanisms 1 and 2 (step$_{1\text{-}1}$ and step$_{2\text{-}1}$, respectively).

In the second step (step$_{3\text{-}2}$, Fig. 19), intermediate I_1 and benzhydrazide with a concerted reaction, pass-through a second transition state ($TS_{3\text{-}2}$) involving three-member ring along with N_1-H bond cleavage and the two H-C_z and N_1-C_z

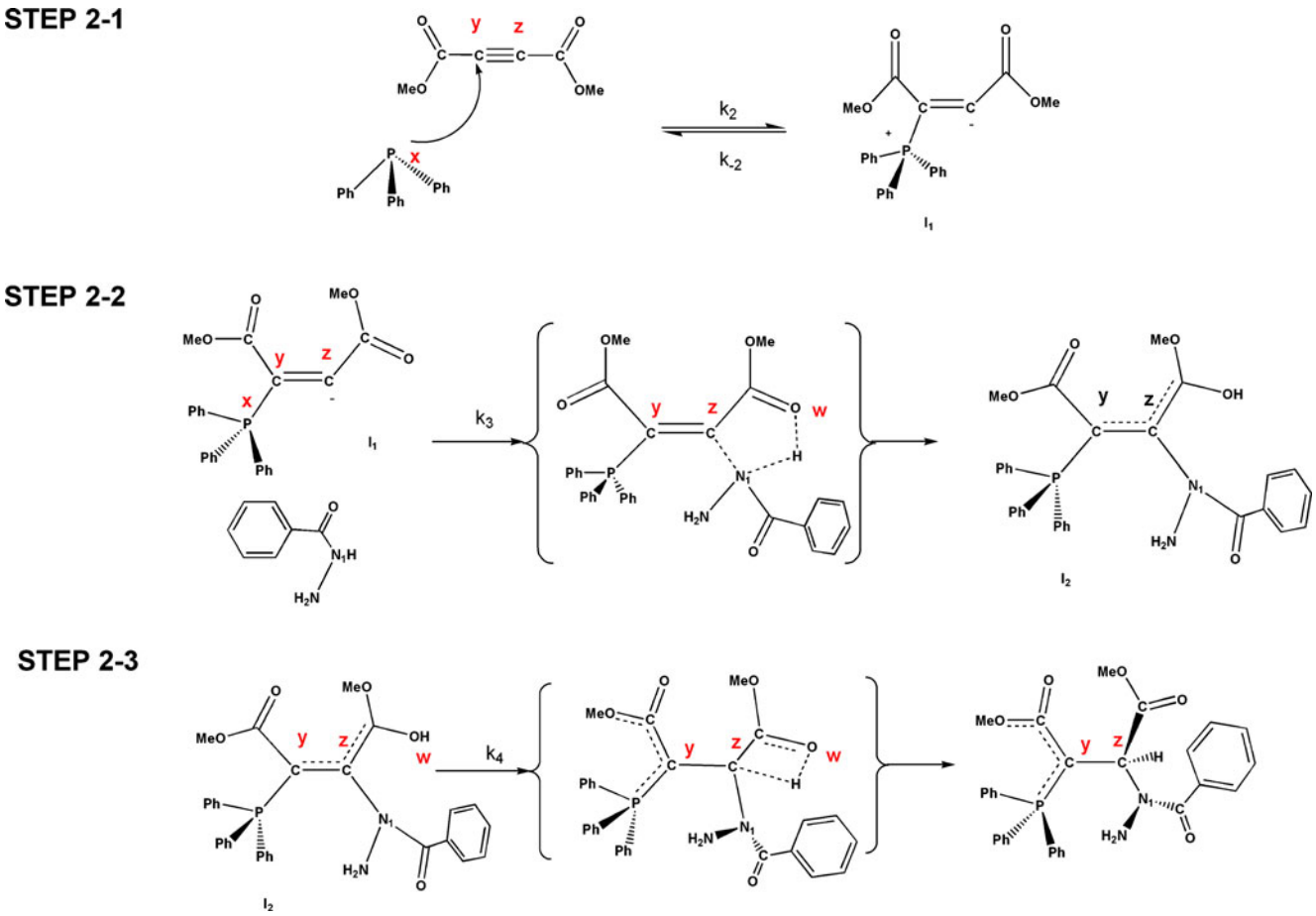

Fig. 18 Speculative proposed mechanism 2 involving three steps for generation of ylide 4

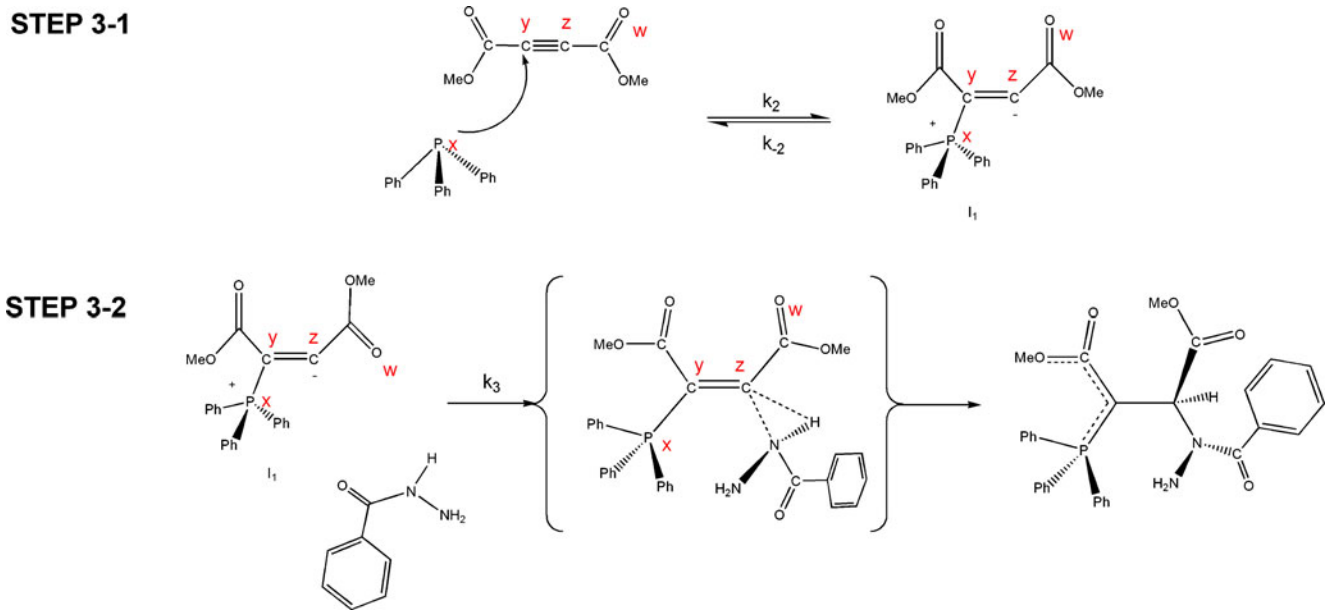

Fig. 19 Speculative proposed mechanism 3 consisting of two steps for generation of ylide 4

bonds formation, instantaneously. Imaginary frequency (1574i cm^{-1}) implies that $TS_{3\text{-}2}$ is a transition state. Activation energy for the two steps of mechanism 3 is 27.90 (k_2) and 33.63 (k_3) kcal mol^{-1}, respectively.

As can be seen, speculative theoretical mechanism 1 was exactly the same as the experimentally proposed kinetic mechanism and can be accepted for the following reasons;

1) First step is rate determining step (Table 8) that is compatible with the first step of experimental kinetic mechanism
2) Also third step (k_3) is a fast step and it is in a good agreement with the experimental kinetic mechanism. In speculative mechanism 3, secound step (k_3) is rate determining step which is not consistent with the experimental results that emphasize on the first step (k_2) as a rate determining step. Mechanism 2 with high activation energy (60 kcal mol^{-1}) in relation to mechanism 1 and 3 is not a rationale suggestion.

Conclusions

Briefly, we have prepared novel phosphorus ylides as hydrazide derivatives with potential peroxidase inhibitors using a one-step reaction between triphenylphosphine 1 and dialkyl acetylenedicarboxylates 2 (2a, 2b or 2c) in the presence of strong NH- acids such as benzhydrazide 3. The present method, carries the advantage that, not only is the reaction performed under neutral conditions, but also the substances can be mixed without any activation or modifications. The benzhydrazide -containing phosphorus ylides 4 (4a, 4b or 4c) may be considered as potentially useful synthetic intermediates. It seems that the procedure described here may be employed as an acceptable method for the preparation of phosphoranes with variable functionalities. In addition, kinetic investigation of these reactions was undertaken by UV. Under the same conditions, activation energy of the reaction with di-tert-butylacetylenedicarboxylate 2c (26.0 kJ mol^{-1}) was higher than the two reactions which were followed by the diethyl acetylenedicarboxylate 2b (15.1 kJ mol^{-1}) and dimethyl acetylenedicarboxylate 2a (10.8 kJ mol^{-1}) in 1,2-dichloroethane. 5. The rate of all reactions were increased in media of higher dielectric constant solvent, this can be related to differences in stabilization of the reactants and the activated complex in transition state by solvent. 6. The more satiric factor in bulky alkyl groups accompanied by its more inductive effect within the structure of dialkyl acetylenedicarboxylate would tend to reduce the rate of overall reactions. 7. With respect to the experimental data, first step of experimentally proposed mechanism was recognized as a rate determining step (k_2) and reaction mechanism was confirmed based upon the obtained experimental results and also steady state approximation.

For confirmation of proposed experimental mechanism, three speculative mechanisms (1, 2 and 3) were proposed on the basis of theoretical calculations. The results indicated that mechanism 1, that was same as the experimental mechanism, is the only acceptable mechanism with the first step (k_2) as a rate determining step. Mechanisms 2 and 3 suggested that (k_4) and (k_3) are rate determining steps, respectively and are in disagreement with the experimental results.

Acknowledgments Authors sincerely thank the University of Sistan & Baluchestan for providing financial support of this work.

References

1. Laszo P (1995) Organic reaction, simplicity and logic. Wiley, New York
2. Johnson AW (1966) Ylied chemistry. Academic, London
3. Cadogan JIG (1979) Organophosphorus reagents in organic synthesis. Academic, New York
4. Engel R (1988) Synthesis of carbon-phosphors bonds. CRC, Boca Raton
5. Hudson HR (1990) In: Hartley FR (ed) The chemistry of organophosphorus compounds; primary, secondary, and tertiary phosphates and heterocyclic organophosphorus (3) compounds. Wiley, New York, pp 382–472
6. Corbridge DEC (1995) Phosphorus: an outline of chemistry, biochemistry and uses. Elsevier, Amsterdam
7. Pietrusiewiz KM, Zablocka M (1994) Chem Rev 94:1375–1411
8. Shen Y (1998) Acc Chem Res 31:584–592
9. Gilchrist TL (1985) Heterocyclic Chemistry. Wiley, NewYork
10. Yavari I, Alizadeh A, Anary-Abbasinejad M (2002) Tetrahedron Lett 43:4503–4505
11. Yavari I, Adib M, Hojabri L (2002) Tetrahedron 58:7213–7219
12. Yavari I, Alizadeh A, Anary-Abbasinejad M (2002) Tetrahedron Lett 43:9449–9452
13. Yavari I, Adib M, Jahani-Moghaddam F, Sayahi MH (2002) Phosphorus Sulfur Silicon Relat Elem 177:545–553
14. Ramazani A, Shajari N, Gouranlou F (2001) Phosphorus Sulfur Silicon Relat Elem 174:223–227
15. Maghsoodlou MT, Habibi-Khorassani SM, Heydari R, Rostami-Charati F (2006) J Chem Res 364-365
16. Maghsoodlou MT, Rostami-Charati F, Habibi-Khorassani SM, Khosroshahrodi M, Makha M (2008) Iran J Chem Chem Eng 27:105–113
17. Maghsoodlou MT, Heydari R, Hazeri N, Habibi-Khorassani SM, Nassiri M, Ghasemzadeh M, Salehzadeh J, Gharechaei Z (2009) Heteroatom Chem 20:240–245
18. Maghsoodlou MT, Hazeri N, Habibi-Khorassani SM, Heydari R, Marandi G, Lashkari M, Bagherpour K, Gharechaei Z (2010) Monatsh Chem 141:351–356
19. Aminkhani A, Kabiri R, Habibi-Khorassani SM, Heydari R, Maghsoodlou MT, Marandi G, Lashkari M, Rostamizadeh M (2009) J Sulfur Chem 30:500–506
20. Habibi-Khorassani SM, Maghsoodlou MT, Zakarianejad M, Nassiri M, Kazemian MA, Karimi P (2008) Heteroatom Chem 19:723–732
21. Ortiz de Montellano PR (1995) Biochimie 77:581–593
22. DePillis GD, Wariishi H, Gold MH, Ortiz de Montellano PR (1990) Arch Biochem Biophys 280:217–223
23. Harris RZ, Wariishi H, Gold MH, Ortiz de Montellano PR (1991) J Biol Chem 266:8751–8758
24. Samokyszyn VM, Ortiz de Montellano PR (1991) Biochemistry 30:11646–11653
25. Burner U, Obinger C, Paumann M, Furtmuller PG, Kettle AJ (1999) J Biol Chem 274:9494–9502
26. Wengenack NL, Rusnak F (2001) Biochemistry 40:8990–8996
27. Torffvit O, Thysell H, Nassberger L (1994) Hum Exp Toxicol 13:563–567
28. Reilly CA, Aust SD (1997) Chem Res Toxicol 10:328–334
29. Silverman RB (1988) Mechanism-based enzyme inactivation: Chemistry and enzymology, vol. 1. CRC, Boca Raton
30. Furtmuller PG, Burner U, Regelsberger G (2000) Biochemistry 39:15578–15584
31. Nielsen OJ, Sehsted J, Langer S, Ljungström E, Wängberg I (1995) Chem Phys Lett 238:359–364
32. Langer S, Ljungström E, Ellemann T, Sehsted J, Nielsen OJ (1995) Chem Phys Lett 53:240–255
33. Petersson GA, Al-Laham MA (1991) J Chem Phys 94:6081–6090
34. Petersson GA, Bennett A, Tensfeldt TG, Al-Laham MA, Shirley WA, Mantzaris J (1988) J Chem Phys 89:2193–2218
35. Becke AD (1988) Phys Rev A 38:3098–3100
36. Lee C, Yang W, Parr RG (1988) Phys Rev B 37:785–789
37. Schmidt MW, Baldridge KK, Boatz JA, Elbert ST, Gordon MS, Jensen JH, Koseki S, Matsunaga N, Nguyen KA, Su SJ, Windus TL, Dupuis M, Montgomery JA (1993) General atomic and molecular electronic structure system. J Comput Chem 14:1347–1363